Comparison of ZF and MF filters through PSLR and ISLR assessment in automotive OFDM radar

Bochra Benmeziane, Jean-Yves Baudais, Stéphane Méric, Kevin Cinglant

Comparison of ZF and MF filters through PSLR and ISLR assessment in automotive OFDM radar

Bochra Benmeziane[*#1], Jean-Yves Baudais[*2] Stéphane Méric[*3] Kevin Cinglant[#4],
[#]ZF Autocruise, Brest, France
[*]Univ Rennes, INSA Rennes, CNRS, IETR-UMR 6164, F-35000 Rennes, France
{[1]bochra.benmeziane, [4]kevin.cinglant}@zf.com, {[2]jean-yves.baudais, [3]stephane.meric}@insa-rennes.fr

***Abstract* — Many filtering strategies can be applied to estimate target position along the range profile in orthogonal frequency-division multiplexing radar. Chief among these filters are the matched filter (MF) and the zero forcing (ZF) method. For each technique, this paper compares the impact on the peak to side lobe ratio (PSLR) and the integrated side lobe ratio (ISLR). The results show that ZF scores higher than MF with respect to PSLR and ISLR in low-noise environments.**

***Keywords* — radar signal processing, matched filters, zero forcing, OFDM.**

I. Introduction

The number of vehicles equipped with radars has been steadily increasing in recent years which led to a higher risk of saturated band [1]. It has then become urgent to investigate detection techniques that can mitigate interference such as Orthogonal Frequency Division Multiplexing (OFDM). OFDM is a multiplexing technique that uses orthogonal sub-carriers to transmit data [2]. This technique can be exploited for radar detection. The estimation of the delay induced by a target range can be performed through a variety of ways exploiting the OFDM signal. Chief among these solutions are matched filter (MF) and zero forcing (ZF). The majority of the current radars operate on a frequency modulated continuous waveform (also known as FMCW). These radars use an MF to estimate the range. MF was also used in the first OFDM radars described in [3]. ZF as a range estimation technique was first introduced by [4]. The interest for this technique came from a desire to perform radar detection and inter-vehicular communication using the same OFDM signal. Both techniques can be used for radar detection. The peak to sidelobe ratio (PSLR) and the integrated sidelobe ratio (ISLR) are crucial in an automotive radar [5]. A high sidelobe might result in a false alarm, causing the vehicle to brake for no reason. Meanwhile, a high general level of sidelobes would raise the threshold above peaks linked to low power echos (farther targets). This would result in an equally dangerous effect.

This paper compares the impact of each technique on the PSLR and the ISLR. Up to our knowledge, ZF and MF as range estimation techniques in OFDM radars have not been compared yet. This paper also highlights the link between ZF and MF for each metric and shows that ZF scores higher in low-noise environments. The rest of the paper is organized as follows. Section II describes the OFDM echo and each range estimation technique. The PSLR and ISLR metrics are then defined and estimated for each technique. The connection between the techniques for each metric is described in Section III. Simulations with respect to different levels of noise are presented in Section IV. Section V finally concludes the paper.

II. Range estimation in OFDM radars

Exploiting an OFDM signal for range estimation has already been thoroughly explored [6], [7]. The OFDM signal uses orthogonal sub-carriers to transmit data through an inverse Fourier transform. The N orthogonal sub-carriers used in an OFDM frame of duration T are $f_n = \frac{n}{T}$, $n \in [0, N-1]$, which guarantees the orthogonality of the sub-carriers. The emitted OFDM symbol is expressed by:

$$\forall t \in [0, T+T_g], x(t) = \frac{1}{\sqrt{N}} \sum_{n=0}^{N-1} a_n e^{2\jmath\pi f_n (t-T_g)} \quad (1)$$

where a_n is the nth emitted complex symbol that has been obtained through any modulation such as M-QAM. The duration T_g of the cyclic prefix is needed by the receiving end for demodulation. The received echo contains distortions due to the environment. The delay due to the distance of the target is then estimated through two different techniques investigated in this paper. One of these techniques exploits the multiplication and convolution property of Fourier transforms to estimate the correlation function of the received echo. This technique is referred to as the MF technique. The other technique is the estimation of the channel through its impulse response. This technique is referred to as ZF.

In the following, the signal is assumed to be narrowband and the duration T is short enough that the Doppler variation within one OFDM symbol is considered to be negligible. The duration T_g is properly sized to absorb the delay. The received and demodulated signal is then [3]:

$$Y(l) = a_l \, e^{\phi} e^{-2\jmath\pi \frac{\tau}{T} l} + W(l) \quad (2)$$

where $\phi = -2\pi\jmath f_c \tau$, f_c is the carrier frequency, τ is the delay of the target, and $W(l)$ is a white Gaussian noise, the variance of which is σ_w^2.

As previously discussed, both techniques can provide a range profile estimation through different methods. For ZF, each $Y(l)$ sample is divided by a_l in order to estimate the

transfer function of the channel. The impulse response is therefore:

$$\chi_{\text{ZF}}(i) = \frac{e^{\phi}}{\sqrt{N}} \sum_{l=0}^{N-1} \frac{Y(l)}{a_l} e^{2\pi\jmath \frac{il}{N}} = \frac{e^{\phi}}{\sqrt{N}} \Big(\sum_{l=0}^{N-1} e^{2\pi\jmath (\frac{iT}{N} - \tau) \frac{l}{T}} + \sum_{l=0}^{N-1} \frac{W(l)}{a_l} e^{2\pi\jmath \frac{il}{N}} \Big) \quad (3)$$

For the MF technique, $Y(l)$ samples are multiplied by a_l. The correlation function is therefore:

$$\chi_{\text{MF}}(i) = \frac{e^{\phi}}{\sqrt{N}} \sum_{l=0}^{N-1} Y(l) \overline{a}_l e^{2\pi\jmath \frac{il}{N}} \quad (4)$$
$$= \frac{e^{\phi}}{\sqrt{N}} \Big(\sum_{l=0}^{N-1} |a_l|^2 e^{2\pi\jmath (\frac{iT}{N} - \tau) \frac{l}{T}} + \sum_{l=0}^{N-1} \overline{a}_l W(l) e^{2\pi\jmath \frac{il}{N}} \Big)$$

with $\overline{a}_l$ denoting the conjugate of a_l. Each of these $\chi(i)$ functions represents a range profile, with peaks at the delays of the detected targets. If $i_\tau = \frac{\tau}{T} N$ is the index of a peak, then:

$$\chi_{\text{ZF}}(i_\tau) = e^{\phi}\sqrt{N} + \frac{e^{\phi}}{\sqrt{N}} \sum_{l=0}^{N-1} \frac{W(l)}{a_l} e^{2\pi\jmath \frac{i_\tau l}{N}} \quad (5)$$

$$\chi_{\text{MF}}(i_\tau) = \frac{e^{\phi}}{\sqrt{N}} \Big(\sum_{l=0}^{N-1} |a_l|^2 + \sum_{l=0}^{N-1} \overline{a}_l W(l) e^{2\pi\jmath \frac{i_\tau l}{N}} \Big) \quad (6)$$

Note that in the following, i_τ is assumed to be integer in order to simplify the analysis. In reality, $\frac{\tau N}{T}$ is often non integer, which causes spectral leakage. This issue can be mitigated by applying a window [8]. With the right window parameters, the analysis applies regardless.

MF was designed to obtain the highest peak SNR possible. Meanwhile, the division by the transmitted symbols a_l in ZF provides range profiles that are independent from these symbols. This allows for the transmission of random symbols, making both inter-vehicle communications and radar detection possible with the same transmitted signal.

III. PSLR AND ISLR CALCULATION AND COMPARISON

Two metrics can be used to characterize the range ambiguity function of the automotive radar. The PSLR is the ratio of the main lobe, identified by $\chi(i_\tau)$, to the highest sidelobe in a range profile. The ISLR is the ratio of the main lobe to the energy of the rest of the range profile. Both PSLR and ISLR are expressed by γ such as:

$$\gamma^2 = \frac{E[|\chi(i_\tau)|^2]}{E\big[\theta\big(\{|\chi(i)|^2\}_{i \neq i_\tau}\big)\big]} \quad (7)$$

where $\theta(\{x_i\}) = \max_i x_i$ for γ_{PSLR} and $\theta(\{x_i\}) = \sum_i x_i$ for γ_{ISLR} [9]. Note that in our case, the sampling frequency is equal to the bandwidth. This means that the main peak is one sample wide. Before we can proceed to compare these metrics for ZF and MF, we need to derive $E[|\chi(i)|^2]$ for both i_τ and $i \neq i_\tau$. With independent and identically distributed noise samples, the expectation of $|\chi(i)|^2$ in (3) leads to:

$$E[|\chi_{\text{ZF}}(i)|^2] = |E[\chi_{\text{ZF}}(i)]|^2 + \sigma_{1/a}^2 \sigma_w^2 \quad (8)$$

where $\sigma_{1/a}^2$ is the variance of $1/a$. This result is obtained with N large enough such that the expectation can be approximated by the average:

$$\sigma_{1/a}^2 = E\left[\frac{1}{a_l^2}\right] = \lim_{N\to\infty} \frac{1}{N} \sum_{i=0}^{N-1} \frac{1}{a_l^2} \quad (9)$$

The values $\sigma_{1/a}^2$ depend on the modulation used and can be tabulated. With MF, the expectation of $|\chi(i)|^2$ in (4) leads to:

$$E[|\chi_{\text{MF}}(i)|^2] = |E[\chi_{\text{MF}}(i)]|^2 + \sigma_a^2 \sigma_w^2 \quad (10)$$

where σ_a^2 is the variance of a_l, also dependent on the modulation used and (10) is obtained with N large enough.

The next step is to compute the squared expectation of the range profile for both i_τ and $i \neq i_\tau$:

$$|E[\chi_{\text{ZF}}(i)]|^2 = \frac{1}{N} \left| \sum_{l=0}^{N-1} e^{2\pi\jmath (\frac{il}{N} - \tau)} \right|^2 + \sigma_{1/a}^2 \sigma_w^2 \quad (11)$$

and

$$|E[\chi_{\text{MF}}(i)]|^2 = \frac{1}{N} \left| \sum_{l=0}^{N-1} |a_l|^2 e^{2\pi\jmath (\frac{il}{N} - \tau)} \right|^2 + \sigma_a^2 \sigma_w^2 \quad (12)$$

In the main lobe, $i = i_\tau$, the squared expectation becomes:

$$|E[\chi_{\text{ZF}}(i_\tau)]|^2 = N + \sigma_{1/a}^2 \sigma_w^2 \quad (13)$$

and

$$|E[\chi_{\text{MF}}(i_\tau)]|^2 = N\sigma_a^4 + \sigma_a^2 \sigma_w^2 \quad (14)$$

Meanwhile, when $i \neq i_\tau$, let α_l defined as $\alpha_l = \frac{|a_l|^2}{\sigma_a^2}$, hence $\forall l, E[\alpha_l] = 1$ and $E[|\alpha_l|^2] \geq 1$. The connection between the squared expectations of ZF and MF for N large enough is:

$$\left| \sum_{l=0}^{N-1} \alpha_l e^{2\pi\jmath (\frac{il}{N} - \tau)} \right|^2 = N(E[\alpha_l^2] - 1) + \left| \sum_{l=0}^{N-1} e^{2\pi\jmath (\frac{il}{N} - \tau)} \right|^2 \quad (15)$$

Consequently, in the case of PSLR, the link between MF and ZF is expressed as:

$$\frac{N + \frac{\sigma_w^2}{\sigma_a^2}}{\gamma_{\text{PSLR,MF}}^2} - \frac{\sigma_w^2}{\sigma_a^2} = \max \alpha_l^2 - 1 + \frac{N + \sigma_{1/a}^2 \sigma_w^2}{\gamma_{\text{PSLR,ZF}}^2} - \sigma_{1/a}^2 \sigma_w^2 \quad (16)$$

In low-noise environments, $\sigma_w^2 \to 0$, and since $\max \alpha_l^2 \geq E[\alpha_l^2] \geq 1$, (16) becomes:

$$\frac{1}{\gamma_{\text{PSLR,MF}}^2} = \frac{\max \alpha_l^2 - 1}{N} + \frac{1}{\gamma_{\text{PSLR,ZF}}^2} \geq \frac{1}{\gamma_{\text{PSLR,ZF}}^2} \quad (17)$$

Table 1. OFDM radar parameters.

Parameter	Notation	Value
Number in sub-carriers	N	1024
Bandwidth	B	375 MHz
Order of M-QAM modulation	M	16
Signal to noise power ratio	SNR $= \frac{\sigma_a^2}{\sigma_w^2}$	20 dB
Carrier frequency	f_c	77 GHz
Target distance	R	12 m

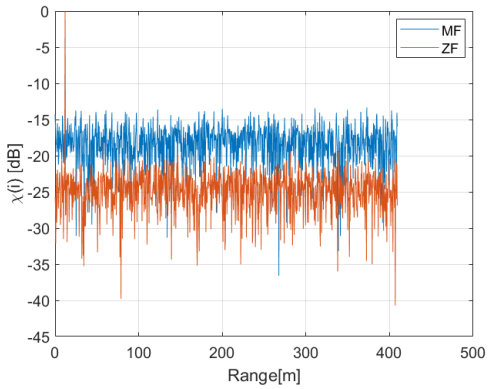

Fig. 1. Normalized range profile comparison.

In the case of ISLR, the link between MF and ZF is expressed as:

$$\frac{N+\frac{\sigma_w^2}{\sigma_a^2}}{\gamma_{\text{ISLR,MF}}}-\frac{\sigma_w^2}{\sigma_a^2}=(N-1)(E[\alpha_l^2]-1)+\frac{N+\sigma_{1/a}^2\sigma_w^2}{\gamma_{\text{ISLR,ZF}}}-\sigma_{1/a}^2\sigma_w^2 \tag{18}$$

and in low noise environments:

$$\frac{1}{\gamma_{\text{ISLR,MF}}^2}=\frac{N-1}{N}(E[\alpha_l^2]-1)+\frac{1}{\gamma_{\text{ISLR,ZF}}^2}\geq\frac{1}{\gamma_{\text{ISLR,ZF}}^2} \tag{19}$$

This shows that for both PSLR and ISLR, ZF performs better in low noise environments.

IV. Results and Discussion

Simulations are performed using the OFDM radar range detection techniques ZF and MF. The OFDM radar system parameters are summarized in Table 1. Using these parameters, together with (3) and (4), the range profiles are estimated and compared in Fig. 1. This figure shows that in a low-noise environment, ZF shows significantly lower levels of sidelobes. However, in order to compare ZF and MF in terms of PSLR and ISLR, further simulations need to be performed in different environments. Using (7), (17) and (19), PSLR and ISLR are computed for each technique. The elements required for this computation are shown in Table 2.

Table 2. QAM parameters.

M	4	8	16	32	64	128	256	512	1024
$E[\alpha_l^2]$	1	1.44	1.32	1.52	1.38	1.54	1.4	1.54	1.4
$\max \alpha_l^2$	1	2.78	3.24	4.98	5.44	6.68	7.01	7.75	7.94

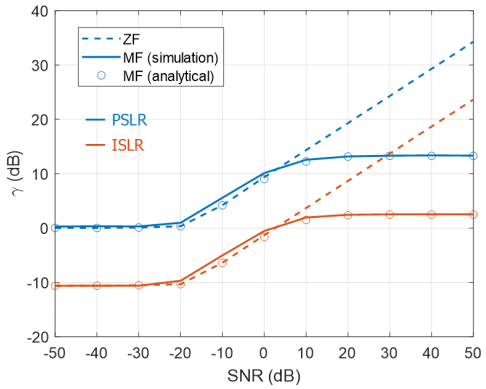

Fig. 2. PSLR and ISLR comparison in different levels of SNR.

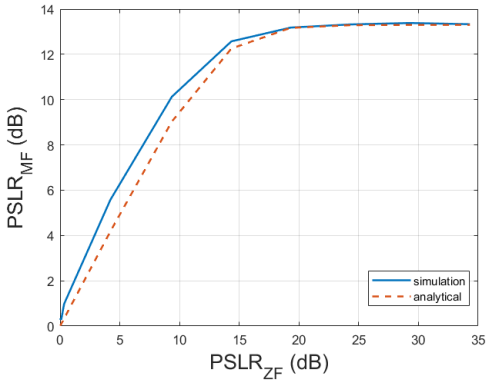

Fig. 3. PSLR comparison in different levels of SNR.

Fig. 2 show the comparison of ZF and MF with $N = 1024$ sub-carriers and using a 16-QAM modulation in different levels of SNR. The simulated plots are computed through (7), while the analytical ones are computed using (17) and (19). The plots show three main trends. In the high end of SNR, (17) and (19) are proven to be accurate, since ZF shows a higher level of PSLR and ISLR, while MF plateaus. For lower SNR, the noise is too high for (17) and (19) to apply. There, MF displays a slightly higher level or PSLR and ISLR. When the SNR < -30 dB, the noise level is too high for detection. The PSLR and ISLR for MF are plotted in terms of PSLR and ISLR for ZF in Fig. 3 and Fig. 4. The figures confirm the previous findings, by showing these metrics steeply escalating for MF before plateauing in low-noise environments.

The main reason that could explain this difference in low-noise environments is the fact that no matter how low the noise gets, the level of the sidelobes due to the correlation function remains unchanged. Whereas, the noise floor of an impulse response depends on the noise only.

The next simulations compare ZF and MF with $N = 1024$ sub-carriers and SNR$= 20$ dB for different orders of M-QAM modulation. The results are plotted in Fig. 5. The figure show that the difference between ZF and MF in their PSLR and ISLR remains virtually unchanged regardless of the order of the used M-QAM modulation and is consistent with the results

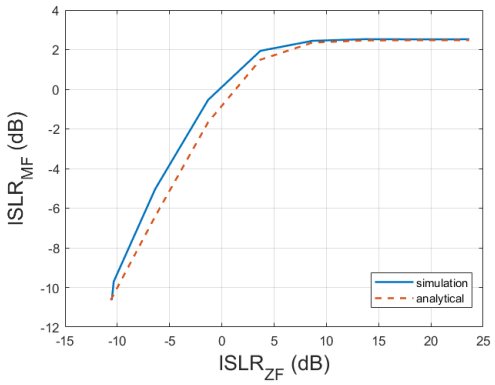

Fig. 4. ISLR comparison for different levels of SNR.

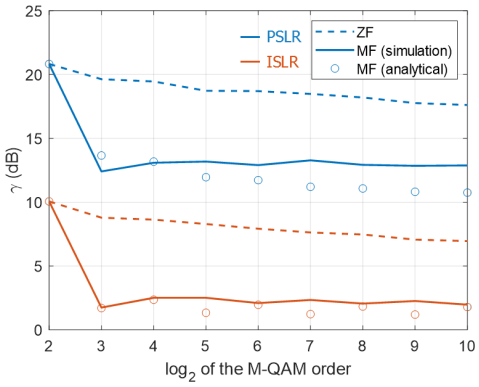

Fig. 5. PSLR and ISLR comparison for different M-QAM orders.

shown in Fig. 2. The notable exception appears for 4-QAM modulation where these metrics are identical for ZF and MF. With this modulation, the modulus of the symbols $|a| = 1$, which means that the range profiles $|\chi_{\text{ZF}}(i)| = |\chi_{\text{MF}}(i)|$.

The last simulation compares ZF and MF using 16-QAM in an environment with SNR $= 20$ dB and for different numbers of sub-carriers.

Once more, Fig. 6 shows the clear superiority of ZF over MF in the PSLR and ISLR departments regardless of the number of orthogonal sub-carriers in a low-noise environment. Hence, it has been proven that for a high SNR level, ZF as a range estimation technique performs better with PSLR and ISLR than MF regardless of the number of sub-carriers or the used modulation. This makes it a better candidate for radar detection in automotive.

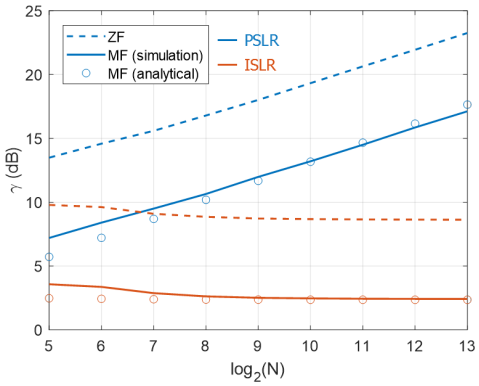

Fig. 6. PSLR and ISLR comparison for different numbers of subcarriers.

V. Conclusion

In this paper, two metrics have been used which are PSLR and ISLR. These two metrics are crucial in an automotive radar. Range estimation techniques which are ZF and MF have been analytically compared on the basis of these two metrics. ZF has proven to be more advantageous in low-noise environments. Simulations have been performed and the superior performances of ZF, which is the considered solution for a joint radar and communication OFDM automotive systems, have been proven.

References

[1] A. Bourdoux, K. Parashar, and M. Bauduin, "Phenomenology of mutual interference of fmcw and pmcw automotive radars," in *2017 IEEE Radar Conference (RadarConf)*. IEEE, 2017, pp. 1709–1714.

[2] T. T. Nguyen, "Design and analysis of superresolution algorithm and signal separation technique for an OFDM-based MIMO radar," 2012.

[3] S. Sen and A. Nehorai, "Adaptive design of OFDM radar signal with improved wideband ambiguity function," *IEEE Transactions on Signal Processing*, vol. 58, no. 2, pp. 928–933, 2009.

[4] C. Sturm, E. Pancera, T. Zwick, and W. Wiesbeck, "A novel approach to OFDM radar processing," in *2009 IEEE Radar Conference*. IEEE, 2009, pp. 1–4.

[5] W. Van Thillo, P. Gioffre, V. Giannini, D. Guermandi, S. Brebels, and A. Bourdoux, "Almost perfect auto-correlation sequences for binary phase-modulated continuous wave radar," in *2013 European Radar Conference*. IEEE, 2013, pp. 491–494.

[6] G. Hakobyan, "Orthogonal Frequency Division Multiplexing Multiple-Input Multiple-Output Automotive Radar with Novel Signal Processing Algorithms," Ph.D. dissertation, Universitat Stuttgart, 2018.

[7] C. Sturm, T. Zwick, and W. Wiesbeck, "An OFDM system concept for joint radar and communications operations," in *VTC Spring 2009-IEEE 69th Vehicular Technology Conference*. IEEE, 2009, pp. 1–5.

[8] F. J. Harris, "On the use of windows for harmonic analysis with the discrete fourier transform," *Proceedings of the IEEE*, vol. 66, no. 1, pp. 51–83, 1978.

[9] X. Lu and H. Sun, "Parameter assessment for SAR image quality evaluation system," in *2007 1st Asian and Pacific Conference on Synthetic Aperture Radar*. IEEE, 2007, pp. 58–60.